Effect of the Cyclobutane Cytidine Dimer on the Properties of *Escherichia coli* DNA Photolyase

Anar K. Murphy,[†] Margaret Tammaro,[§] Frank Cortazar,[§] Yvonne M. Gindt,[§] and Johannes P. M. Schelvis*[,†,‡,⊥]

Department of Chemistry, New York University, 100 Washington Square East, New York, New York 10003; Department of Chemistry and Biochemistry, Montclair State University, 1 Normal Avenue, Montclair, New Jersey 07043; and Department of Chemistry, Lafayette College, Hugel Science Center, Easton, Pennsylvania 18042

Received: July 23, 2008; Revised Manuscript Received: September 18, 2008

Cyclobutane pyrimidine dimer (CPD) photolyases are structure specific DNA-repair enzymes that specialize in the repair of CPDs, the major photoproducts that are formed upon irradiation of DNA with ultraviolet light. The purified enzyme binds a flavin adenine dinucleotide (FAD), which is in the neutral radical semiquinone ($FADH^{\bullet}$) form. The CPDs are repaired by a light-driven, electron transfer from the anionic hydroquinone ($FADH^{-}$) singlet excited state to the CPD, which is followed by reductive cleavage of the cyclobutane ring and subsequent monomerization of the pyrimidine bases. CPDs formed between two adjacent thymidine bases (T<>T) are repaired with greater efficiency than those formed between two adjacent cytidine bases (C<>C). In this paper, we investigate the changes in *Escherichia coli* photolyase that are induced upon binding to DNA containing C<>C lesions using resonance Raman, UV−vis absorption, and transient absorption spectroscopies, spectroelectrochemistry, and computational chemistry. The binding of photolyase to a C<>C lesion modifies the energy levels of $FADH^{\bullet}$, the rate of charge recombination between $FADH^{-}$ and $Trp_{306}^{\bullet}$, and protein−$FADH^{\bullet}$ interactions differently than binding to a T<>T lesion. However, the reduction potential of the $FADH^{-}/FADH^{\bullet}$ couple is modified in the same way with both substrates. Our calculations show that the permanent electric dipole moment of C<>C is stronger (12.1 D) and oriented differently than that of T<>T (8.7 D). The possible role of the electric dipole moment of the CPD in modifying the physicochemical properties of photolyase as well as in affecting CPD repair will be discussed.

Introduction

Ultraviolet (UV) light is one of the most common environmental sources of DNA damage, and the solar radiation that reaches the earth's surface produces two significant photoproducts of DNA by photodimerization of adjacent pyrimidine bases:[1−3] the cyclobutane pyrimidine dimer (CPD) and the pyrimidine-(6-4)-pyrimidone photoproduct. The CPD is the most prevalent and the most mutagenic of the two.[1−4] Although the CPD of two thymidines (T<>T) has the highest rate of occurrence,[5] the CPD of two cytidines (C<>C) poses an additional problem. Cytidine can undergo deamination to uridine, but the deamination process is slow for unmodified cytidine.[6] In the C<>C, the deamination process is accelerated dramatically, and the final result is a CC to TT tandem mutation, a lesion directly linked to skin cancer.[7−9] In mammals, the main repair mechanism of CPDs is nucleotide excision repair (NER) which requires about 30 proteins for the removal of bulky lesions from DNA.[10] Despite repair by the NER mechanism, the half-life of CPDs in mammals is about 24 h, and CPDs can still be detected up to 3 weeks after irradiation of skin with UV light.[11] Many organisms, though not placental mammals, possess CPD photolyases, structure-specific DNA repair enzymes that use a light-driven, electron-transfer mechanism to repair CPDs very efficiently.[12] There is a separate (6-4)-photolyase that repairs the (6-4)-photoproduct.

Photolyases are flavoenzymes that contain a flavin adenine dinucleotide (FAD) in the active site which has to be in its anionic hydroquinone form ($FADH^{-}$) to be active in DNA repair.[12] *Escherichia coli* possesses only a CPD-photolyase, the most widely studied photolyase. Besides the FAD cofactor, the enzyme binds 5,10-methenyltetrahydrofolate polyglutamate (MTHF), which acts as a light-harvesting pigment.[13] After isolation and purification of the enzyme, the FAD cofactor has oxidized to a stable neutral radical semiquinone, $FADH^{\bullet}$, an inactive form of the enzyme.[14−17] Photolyase can undergo two light-driven, electron-transfer processes: DNA repair through photoreactivation in vivo and photoreduction of $FADH^{\bullet}$ in vitro.[12,18] In photoreduction, the excited $FADH^{\bullet}$ is reduced by the nearby Trp_{382}.[19,20] Trp_{382} has been proposed to be the first tryptophan in a chain of three tryptophans that participate in the photoreduction process, but the exact pathway of photoreduction is still under debate.[19−21] Trp_{306} is the terminal electron donor, and charge recombination between $FADH^{-}$ and $Trp_{306}^{\bullet}$ occurs on the millisecond time scale.[15,16,22,23] The photoreduction process observed in vitro may not play a physiological role.[24]

The crystal structures of CPD photolyases from various organisms show that the FAD cofactor sits at the bottom of a cavity that extends to the protein surface.[25−27] It was proposed that the CPD would flip out of the duplex DNA and into this cavity, bringing it in close proximity of the FAD cofactor.[25] Computer modeling and various experimental studies provided

* Corresponding author: Tel +973 655 3301, Fax 973 655 7772, e-mail schelvisj@mail.montclair.edu.
[†] New York University.
[‡] Montclair State University.
[§] Lafayette College.
[⊥] Current address: Department of Chemistry and Biochemistry, Montclair State University, 1 Normal Avenue, Montclair, NJ 07043.

10.1021/jp806526y CCC: $40.75
Published on Web 10/31/2008

supporting evidence for a flipped-out substrate binding geometry.[28−33] The crystal structure of *A. nidulans* photolyase with a repaired CPD analogue in the proposed substrate binding cavity indicates that the CPD binds very close to the FAD cofactor, forming hydrogen bonds with the adenine unit and potentially in van der Waals contact with its 8-methyl group.[34]

MacFarlane and Stanley were the first to propose that the permanent electric dipole moment of the CPD may affect the properties of the FAD cofactor on the basis of a blue shift in the FAD absorption spectrum upon binding of photolyase to T<>T-containing DNA.[31] We observed a similar blue shift in the absorption spectrum of $FADH^{\bullet}$ when photolyase binds to T<>T-containing DNA.[35] We have also measured a decrease in the charge recombination rate following photoreduction of $FADH^{\bullet}$.[36] More importantly, substrate binding seems to modify interactions between the FAD cofactor and its protein environment and is responsible for an increase in the $FADH^{-}/FADH^{\bullet}$ reduction potential, which may serve to stabilize the active, $FADH^{-}$ form of the enzyme by a factor of 10 under aerobic conditions.[35,37]

The dipole moment of cytosine is stronger than that of thymine,[38,39] and experiments on the photolyase bound C<>C-containing DNA will shed light on the role of the dipole moment on the increased photolyase repair efficiency for T<>T in relation to C<>C lesions.[40] In this paper, we investigate the effect of the electric dipole moment of the C<>C CPD on the properties of photolyase for comparison to those induced by the T<>T CPD. We use semiemperical AM-1, ab initio Hartree−Fock, and density functional theory (DFT) methods to calculate the strength and orientation of the electric dipole moment of cytidine, uridine, and thymidine CPDs. We also use a UV-damaged cytidine decamer to investigate the effect of the cytidine CPD on the properties of $FADH^{\bullet}$ in *E. coli* photolyase as measured by UV−vis absorption, nanosecond transient absorption, and resonance Raman spectroscopies and by spectroelectrochemistry. The calculations predict very similar electric dipole moments for the thymidine and uridine CPDs while the cytidine CPD is predicted to have a significantly larger electric dipole moment with a different orientation. The cytidine CPD modifies the absorption spectrum of $FADH^{\bullet}$ and the charge recombination kinetics in *E. coli* photolyase differently than the thymidine CPD, and these results can be explained qualitatively by the differences in their electric dipole moments. Furthermore, binding of the cytidine CPD induces smaller changes in the resonance Raman spectrum of $FADH^{\bullet}$ along with a similar calong withhange in the $FADH^{-}/FADH^{\bullet}$ reduction potential compared to the thymidine CPD. These results will be discussed in light of the different repair efficiencies of photolyase for T<>T and C<>C lesions.

Materials and Methods

Materials. All chemicals were purchased from Sigma-Aldrich and were used without further purification. The polythymidylate and polycytidylate decamers, $p(dT)_{10}$ and $p(dC)_{10}$, were purchased from TriLink BioTechnologies (San Diego) in crude, desalted form.

Enzyme Overexpression and Purification. *E. coli* strain pMS969 was a generous gift from Dr. A. Sancar (University of North Carolina). Cells were grown and harvested and DNA photolyase was overexpressed and purified as described previously.[15,35] The purified enzyme was stored in 50 mM HEPES pH 7.0 and 0.4 M K_2SO_4 or in 20 mM potassium phosphate pH 7.0 and 0.4 M K_2SO_4 at −80 °C.

Substrate Preparation. The $p(dC)_{10}$ and $p(dT)_{10}$ were purified by HPLC (PU-987, Jasco Inc.) on a reverse-phase Microsorb-MV column (C18, 250−4.6 mm, 100 Å, Varian Inc.). For purification, solutions of 2 mM $p(dC)_{10}$ or 2 mM $p(dT)_{10}$ in water were eluted with a 40 min, 0−12% acetonitrile gradient. All the water that was used was passed through deionization and organic removal columns and distilled with a MegaPure system (Barnstead). A rotary evaporator was used to remove acetonitrile from the purified oligonucleotide fractions and to concentrate them to their initial concentrations. The $p(dC)_{10}$ and $p(dT)_{10}$ solutions were placed in quartz cuvettes, which were purged with nitrogen gas for 30 min and sealed with rubber septa. The cuvettes were placed on ice and irradiated with 254 nm light (6 W, UV-B/C, Spectroline) to induce CPD lesions. For the absorption and electron transfer experiments, 1 mM $p(dC)_{10}$ and 1 mM $p(dT)_{10}$ and 2 mM $p(dC)_{10}$ and 0.7 mM $p(dT)_{10}$, respectively, in 0.4 M K_2SO_4, 50 mM HEPES at pH 7.0 were irradiated. For the resonance Raman experiments, 6 mM $p(dC)_{10}$ in 0.4 M K_2SO_4, 20 mM potassium phosphate at pH 7.0 was irradiated. The phosphate buffer was used because the HEPES buffer gave rise to a luminescent background in the resonance Raman experiments. The progress of DNA damage was monitored by the ratio of the $p(dT)_{10}$ and $p(dC)_{10}$ absorbance at 265 and 270 nm, respectively, and the absorbance of their (6-4)-photoproduct at 325 nm. An A_{265}/A_{325} ratio between 20 and 25 is optimal for the formation of ∼1.5 CPD/oligonucleotide (Pun, D.; Schelvis, J. P. M., unpublished results). The time required for the formation of the C<>C lesions was significantly longer than that of the T<>T lesions, in agreement with the literature.[5] UV-damaged $p(dT)_{10}$ and $p(dC)_{10}$ (UV-$p(dT)_{10}$ and UV-$p(dC)_{10}$) were not further purified because of the high affinity of *E. coli* photolyase for the CPD photoproduct compared to the (6-4)-photoproduct.[41] UV-$p(dT)_{10}$ and UV-$p(dC)_{10}$ were stored at −80 °C to prevent spontaneous deamination of the C<>C lesions.[8]

Electronic Absorption Spectroscopy. The electronic absorption spectra were recorded on a UV−vis spectrophotometer (Lambda P40, Perkin-Elmer) at room temperature and at 4 °C. To obtain a high photolyase:UV-$p(dC)_{10}$ ratio and to monitor the absorption changes as a function of UV-$p(dC)_{10}$ concentration, a starting solution of 60 μM photolyase was diluted by addition of aliquots of the concentrated UV-$p(dC)_{10}$ solution to a final enzyme concentration of 20 μM with 30-fold excess of UV-$p(dC)_{10}$. The absorption spectra were converted to an energy scale and deconvoluted with a set of normalized Gaussians of the form $G(x) = [A/(w(\pi/2)^{1/2})]\ \exp\{-2[(x - x_0)^2/w^2]\}$ where A is the area, w is the width, and x_0 is the position of the Gaussian. The deconvolution procedure has been described previously and was performed with Origin 7.0 (OriginLab Corp.).[35]

Resonance Raman Spectroscopy. The resonance Raman spectra were collected on a system that has been described before.[35] Each sample (200 μL of 200 μM photolyase) was placed in a Raman spinning cell sealed with a rubber septum. The samples were excited with 20 mW of 532 nm light from a diode-pumped solid-state laser (LambdaPro Technologies Ltd.). The spinning cells were placed in a chamber that was cooled to 6 ± 2 °C with nitrogen gas that was passed through an acetone/dry ice bath. The absorption spectra of photolyase before and after laser irradiation were nearly identical. Only a minor contribution from oxidized photolyase was detectable in the absorption spectrum, and no vibrations due to oxidized FAD were observed in the resonance Raman spectra because of selective enhancement of $FADH^{\bullet}$. The resonance Raman spectra

were calibrated with the toluene and corrected for a sloping background with a smooth polynomial function.

Electron Transfer Experiments. The electron transfer experiments on DNA photolyase and its complex with UV-p(dC)$_{10}$ and UV-p(dT)$_{10}$ were performed at pH 7.0 on a kinetic spectrophotometer system (7 ns response time) that was described previously.[36] For each sample, six single-shot transient absorption traces were measured at 510, 560, 580, and 625 nm after excitation of the samples at 532 nm. The experiments were conducted at room temperature, and the steady-state absorption spectra taken immediately after the laser flash photolysis confirmed substrate binding to photolyase. The charge recombination kinetics were analyzed using Origin 7.0 (OriginLab Corp.).

Reduction Midpoint Potential Titrations. The reduction potential of the enzyme in the presence of substrate was measured as described previously with the following modification; the buffer system was changed to 0.40 M K_2SO_4 with 0.050 M potassium phosphate buffer, pH 7.0.[37] All data were acquired at 10 °C, and all solutions were made just prior to measurement. The ratio of substrate to enzyme ranged from 10:1 to 25:1 with no discernible change in the measured reduction potential.

Calculations. Semiempirical AM1 and ab initio Hartree−Fock (HF) calculations were carried out with the Spartan 4.0 software package (Wave function, Inc.) on a PC. Density functional theory (DFT) level calculations were performed by using the B3LYP functional and the 6-31G(d,p) basis set in the Gaussian 98 software package, using an Origin200 microcomputer (Silicon Graphics) at the Academic Computing Services, New York University. The initial structure of each molecule was built using Spartan 4.0, and their optimized geometries were first calculated at the AM1 level. This AM1-optimized geometry was used as the starting structure for geometry reoptimization at the HF level with the 3-21G* basis set. Each HF-optimized structure served as input for the DFT-level geometry reoptimization of each molecule. At each level of computational methodology, the ground-state electric dipole moment of each molecule was calculated.

Results

Effect of C<>C on the Electronic Absorption Spectrum of FADH•. The electronic absorption spectrum of *E. coli* photolyase is shown in Figure 1. The spectrum is characterized by the absorption bands of FADH• at 496, 584, and 623 nm.[14,15] The strong absorption band at 383 nm is mainly due to the MTHF cofactor with a minor contribution of FADH•.[42] A 12-fold molar excess of UV-p(dC)$_{10}$ was found to be sufficient to form the enzyme−substrate, as judged from the changes in the UV−vis absorption spectrum with titration of 30-fold excess of substrate. This ratio is about 10-fold higher than the UV-p(dT)$_{10}$-to-photolyase ratio that is necessary to form the enzyme−substrate complex, in agreement with earlier findings.[40] The small but reproducible changes in the FADH• absorption spectrum upon addition of UV-p(dC)$_{10}$ are evidence for the formation of the enzyme−substrate complex under our experimental conditions. The absorbance changes that are induced by binding of photolyase to 3-fold excess UV-p(dT)$_{10}$ are shown in the inset of Figure 1 for comparison. A small blue shift of the two main absorption bands can be observed upon binding to the UV-p(dC)$_{10}$ substrate as well as a small decrease in the extinction coefficient of both the $D_0 \rightarrow D_1$ and the $D_0 \rightarrow D_2$ transition. The latter is in contrast with the binding of UV-p(dT)$_{10}$, which causes an increase and a decrease in the extinction coefficient of the $D_0 \rightarrow D_1$ and the $D_0 \rightarrow D_2$ transitions, respectively. The large increase in absorbance below 380 nm is due to a slight contamination of the cytidine (6-4)-photoproduct.

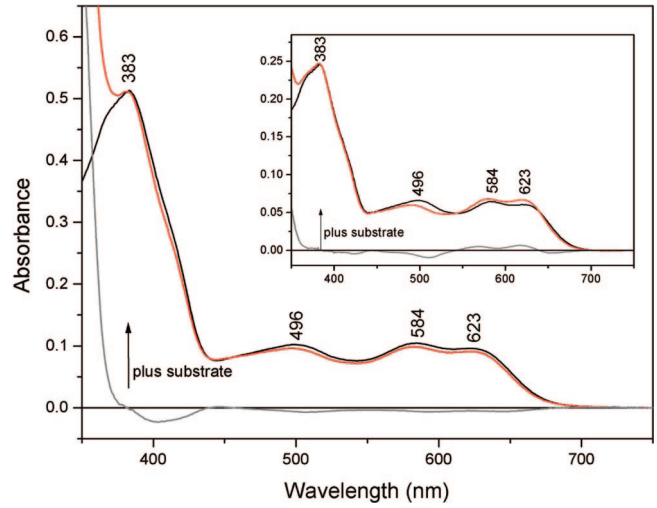

Figure 1. Absorption spectra of *E. coli* photolyase in the absence (black line) and presence of 25-fold excess of UV-p(dC)$_{10}$ (red line). The final enzyme concentration was 20 μM. The gray line represents the difference spectrum (substrate-bound minus substrate-free). Inset: absorption spectra of *E. coli* photolyase in the absence (black line) and presence of 8-fold excess of UV-p(dT)$_{10}$ (red line). The final enzyme concentration was 14 μM.

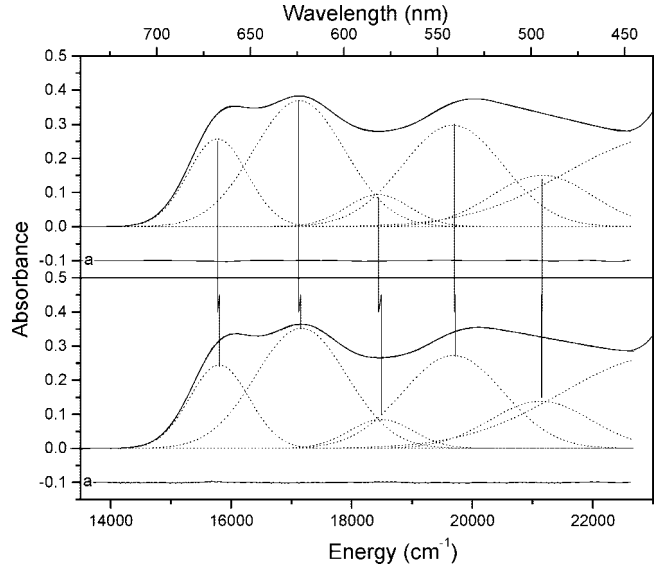

Figure 2. Deconvolution of the absorption spectrum of FADH• in *E. coli* photolyase in the absence (A) and presence (B) of UV-p(dC)$_{10}$. The dotted lines labeled 1 through 6 represent the Gaussian bands obtained from the deconvolution procedure. The vertical lines have been added to visualize the shift of each Gaussian band. The residuals are shown at the bottom of each graph.

To quantify the electrochromic shift of the electronic transitions of FADH• in photolyase upon binding to UV-p(dC)$_{10}$, the absorption spectra were converted to an energy scale and deconvoluted with Gaussian bands as was previously described.[35] The results for one set of spectra are shown in Figure 2. Analysis of all the data shows that the $D_0 \rightarrow D_1$ transition of FADH• undergoes a 30 ± 2 cm^{-1} blue shift upon binding of photolyase to UV-p(dC)$_{10}$. This shift is 2.5 times smaller than the one that is observed upon binding of the enzyme to UV-p(dT)$_{10}$.[35] The results of the fit can be found in the Supporting Information (Table S1).

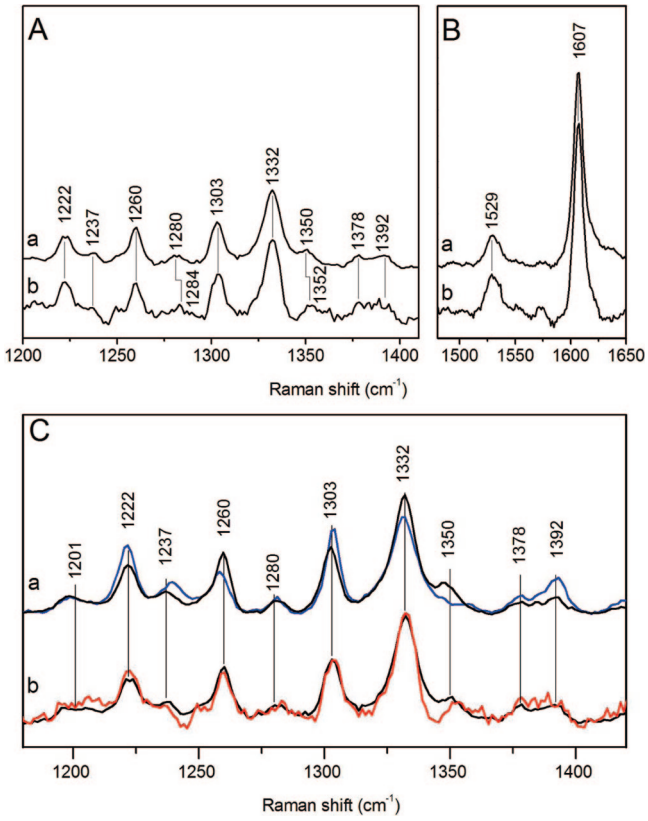

Figure 3. (A and B) Resonance Raman spectra of *E. coli* photolyase in the absence (a) and presence (b) of UV-p(dC)$_{10}$ and (C) of *E. coli* photolyase in the absence (black) and presence (red) of UV-p(dC)$_{10}$ and in the presence (blue) of UV-p(dT)$_{10}$ (top spectra adapted from ref 35). Excitation was at 532 nm with 20 mW.

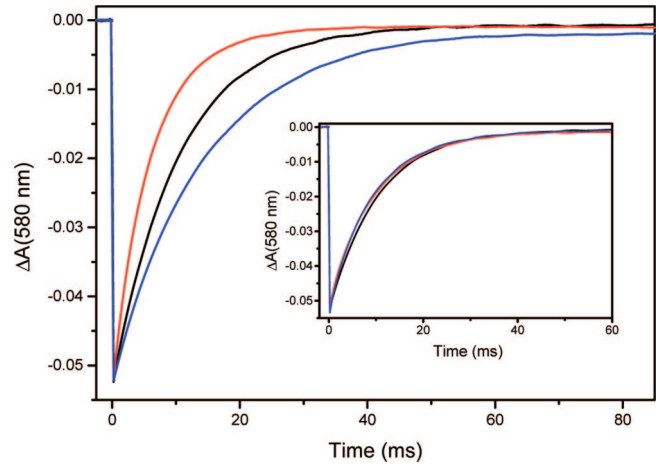

Figure 4. Transient absorption changes at 580 nm for *E. coli* photolyase (black) and its complex with UV-p(dC)$_{10}$ (red) and with UV-p(dT)$_{10}$ (blue) at pH 7.0. Inset: *E. coli* photolyase in the absence (black) and presence (red) of undamaged p(dC)$_{10}$ and in the presence of undamaged p(dT)$_{10}$ (blue) at pH 7.0.

TABLE 1: Effect of Substrate Binding on the Properties of *E. coli* Photolyase and Its FADH• Cofactor

sample	τ (ms)[a]	ΔE (cm^{-1})[b]	E_m(FADH$^-$/FADH•) (mV)	dipole moment (D)
photolyase	10.1 ± 0.1		+16 ± 6[e]	
	10.2 ± 0.3[c]			
+ C[*c,s*]C	7.1 ± 0.6	30 ± 2	+87 ± 15	16.0[f]
+ T[*c,s*]T	14.4 ± 0.5	82 ± 8[d]	+81 ± 8[e]	8.7[f]
	17.8 ± 0.4[c]			

[a] Charge recombination time. [b] ΔE = electrochromic shift. [c] Reference 36. [d] Reference 35. [e] Reference 37. [f] CPD III, calculated with HF 3-21G*.

Effect of C<>C on FADH•−Protein Interactions. Resonance Raman spectroscopy was instrumental in identifying the perturbation of protein−FADH• interactions upon binding of photolyase to UV-p(dT)$_{10}$.[35] The resonance Raman spectra of FADH• in *E. coli* photolyase in its free and UV-p(dC)$_{10}$ bound forms excited at 532 nm are shown in Figure 3. The redox marker band of FADH• in photolyase occurs at 1607 cm^{-1}, in agreement with previous studies,[35,43,44] and other strong bands are observed at 1529, 1332, 1303, 1260, and 1222 cm^{-1} (Figure 3A,B). The use of phosphate buffer ensured that no buffer contributions were observed above 1000 cm^{-1}. The weak band at 1638 cm^{-1} is associated with a normal mode of the MTHF cofactor.[42] Despite the HPLC purification step, addition of 12-fold excess of UV-p(dC)$_{10}$ gave rise to a luminescent background, and the quality of the resonance Raman spectrum of FADH• in the photolyase-UV-p(dC)$_{10}$ complex is relatively poor. For comparison, the resonance Raman spectra of photolyase in the absence and presence of UV-p(dT)$_{10}$ and of UV-p(dC)$_{10}$ are shown in Figure 3C. The results of the control experiment with UV-p(dT)$_{10}$ are consistent with previously reported data.[35] The addition of UV-p(dC)$_{10}$ induces smaller changes in the FADH• spectrum than UV-p(dT)$_{10}$. The largest change is observed for the band at 1350 cm^{-1} which appears to shift to 1353 cm^{-1}. The frequency shift suggests that binding of UV-p(dC)$_{10}$ to photolyase still causes a change in hydrogen bonding between FADH• and its protein environment but to a lesser extent than that observed with UV-p(dT)$_{10}$.[35]

Effect of C<>C on Charge Recombination from FADH$^-$ to Trp$_{306}$•. Photoreduction of FADH• to FADH$^-$ is observed as bleaching of the FADH• ground-state absorption which recovers during the charge-recombination process when FADH• is re-formed. Typical charge-recombination kinetics between FADH$^-$ and Trp$_{306}$• in free enzyme and in the complex with UV-p(dC)$_{10}$ and UV-p(dT)$_{10}$ as monitored at 580 nm at pH 7.0 are shown in Figure 4. The kinetic traces observed at 510, 560, and 625 nm show similar decay kinetics though different amplitudes (data not shown). The transient absorption traces were fit to a monoexponential decay function, and the time constants for charge recombination are listed in Table 1. The fits and residual plots can be found in the Supporting Information. The charge-recombination kinetics in the photolyase−UV-p(dT)$_{10}$ complex become faster after the first three excitation pulses and with each subsequent pulse slowly approached the time constant that was measured for the free enzyme; therefore, only the first three measurements of each of these samples were used in the data analysis. It appears that a small amount of fully reduced photolyase builds up in the solution and repairs the UV-p(dT)$_{10}$. A similar repair of CPD lesions with FADH• photolyase was reported before.[16] No repair of UV-p(dC)$_{10}$ was observed during the transient absorption experiments due to the significantly lower repair efficiency of photolyase for this substrate.[40]

The data in Figure 4 clearly demonstrate that the time required for charge recombination in photolyase decreases in the presence of UV-p(dC)$_{10}$ and increases in the presence of UV-p(dT)$_{10}$. The time constant is 10.1 ± 0.1 ms for photolyase alone, 7.1 ± 0.6 ms for the photolyase−UV-p(dC)$_{10}$ complex, and 14.3 ± 0.4 ms for the photolyase−UV-p(dT)$_{10}$ complex. The latter time constant is slightly smaller than the one obtained previously[36] and may be attributed to the strong influence of pH on the charge-recombination process.[19,36,45] Control experiments on

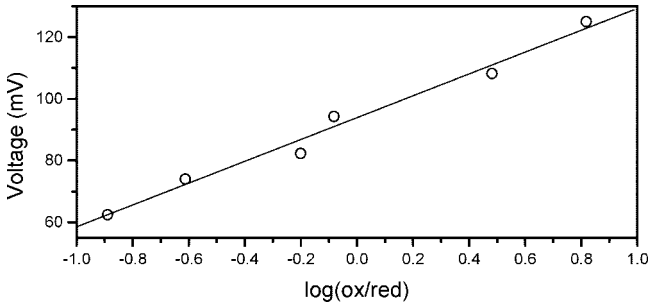

Figure 5. Typical Nernst plot of the spectroelectrochemical titration of the $FADH^-/FADH^\bullet$ couple in *E. coli* photolyase in the presence of UV-p$(dC)_{10}$. The straight line is the best fit through the data.

photolyase in the presence of 28-fold excess undamaged d$(pC)_{10}$ or 10-fold excess undamaged d$(pT)_{10}$ showed no change in the charge-recombination kinetics from free enzyme (Figure 4, inset). A pH-dependent study of the photolyase−UV-p$(dC)_{10}$ complex was not done due to the rapid deamination of C<>C lesions at pH values below and above 7.0.[8]

Effect of C<>C on the $FADH^-/FADH^\bullet$ Reduction Potential in Photolyase. Figure 5 shows the Nernst plot of the electrochemical titration for the reduction of $FADH^\bullet$ in photolyase. The concentration of $FADH^\bullet$ was determined from the 580 nm absorbance using an extinction coefficient of 4800 M^{-1} cm^{-1}.[46] The $FADH^-/FADH^\bullet$ reduction potential of the enzyme in the presence of UV-p$(dC)_{10}$ was found to be 87 ± 15 mV vs NHE. Earlier, we measured the reduction potential of the free enzyme and enzyme with UV-p$(dT)_{10}$ substrate to be 16 ± 6 and 81 ± 8 mV, respectively.[37]

Calculation of the Electric Dipole Moment. To obtain better qualitative and quantitative understanding of the different effects of the permanent dipole moments of the C<>C and T<>T lesions on the properties of *E. coli* photolyase, we have calculated the electric dipole moments of the pyrimidine nucleobases, nucleosides, and nucleotides along with the dipole moments of their various *cis,syn*-cyclobutane dimers. To characterize the contribution of structural features to the electric dipole moment, the electric dipole moments were calculated in the absence and presence of the sugar and phosphate groups, and eight different structures were analyzed for each pyrimidine. The results of the Hartree−Fock (HF) calculations are summarized in Table 2.

The calculated dipole strengths of thymine, uracil, and cytosine at the HF level are in very good agreement with those that have been previously reported at the same level of theory.[47−50] They predict the experimental value of the dipole strength of the cytosine nucleobase and of the thymine and uracil nucleosides very well.[38,39] They also predict that the dipole moment of each pyrimidine becomes stronger in going from nucleobase to nucleoside to nucleotide, which is in agreement with experimental observations for the nucleobase and nucleoside.[38,39] Interestingly, the electric dipole moment of cytosine is 1.5 times stronger than those of thymine and uracil, which have similar strengths.

Neither experimental nor computational data are available for the electric dipole moment of the CPD, though the value of T<>T has been estimated to be about 8.0 D when bound to photolyase.[31] To estimate the electric dipole moment of the substrate upon binding to photolyase, we analyzed two CPD dinucleotides with phosphates on each pyrimidine with a broken (CPD I) and intact (CPD II) phosphate−sugar bond between the pyrimidines along with a third CPD dinucleotide with only one phosphate group forming the phosphate−sugar bond between the pyrimidines (CPD III). The structures of these CPDs can be found in the Supporting Information. Assuming that the phosphate groups on the 5′- and 3′-side of the CPD are neutralized by interactions with positively charged amino acids at the rim of the binding pocket, the latter structure is as close as possible to the CPD structure in the enzyme−substrate complex.[28,33,34] The major trend predicted by the calculations is that the dipole moments of the various CPD structures strengthen from uracil to thymine to cytosine, with the latter having a significantly larger dipole moment. It is also predicted that the addition of the sugar group and subsequently the phosphate group to each pyrimidine increases the strength of the electric dipole moment. Addition of the phosphate link between the two pyrimidines (CPD II) causes a 1.2-fold increase in the strength of the dipole moment for the thymine and uracil dimers, but a 10% decrease is calculated for the cytosine dimer. Removal of the external phosphate group (CPD III), leaving only the linking phosphate, causes a decrease in the strength of the electric dipole moment of about 40%. The resulting dipole moment has twice the strength of that of a single nucleobase. The calculated dipole strength of CPD III is surprisingly close to the value that was estimated by MacFarlane and Stanley for the enzyme−substrate complex,[31] even though our calculations are done in vacuum.

Besides using the HF method, we also calculated the dipole moments with the AM1 and DFT methods. The results of all these calculations can be found in the Supporting Information. The correctness of the calculated electric dipole moment strength relies heavily on the optimized geometry of the CPD structures. Published optimized structures of CPDs and the crystal structure of DNA containing a CPD clearly show a puckered, nonplanar cyclobutane ring.[51−54] The AM1 method consistently returns optimized CPD geometries that contain a planar cyclobutane ring, while those calculated with the HF and DFT methods do return a puckered cyclobutane ring and result in nearly identical structures. However, the DFT calculations predict significantly lower values for the strength of the electric dipole moments of CPD III, and its values for the nucleosides deviate from experimental values (see Supporting Information). Since the AM1 calculations give the incorrect CPD structure and the DFT calculations give dipole moment values that are too different from experimental values, we will use the electric dipole

TABLE 2: Electric Dipole Moment Strength (in D) for Thymine (T), Uracil (U), Cytosine (C), and Various of Their *cis,syn*-Cyclobutane Dimers (Hartree−Fock, 3-21G*)

	experimental values[a]		
	T	U	C
nucleobase	4.1	4.2	7.0
nucleoside	5.25	5.25	n.a.[b]
	monomer	monomer	monomer
nucleobase	4.65	4.79	7.15
nucleoside	5.30	5.25	8.35
nucleotide	7.11	7.5	13.76
	dimer	dimer	dimer
nucleobase	7.35	7.15	12.12
nucleoside	10.02	9.70	13.44
CPD I[c]	14.2	13.88	19.93
CPD II[d]	17.69	17.14	17.67
CPD III[e]	8.67	8.13	16.04

[a] Experimental values were taken from refs 38 and 39. [b] n.a. = not available. [c] CPD I: dimer of nucleotides without inter pyrimidine phosphate−sugar link. [d] CPD II: dimer of nucleotides with interpyrimidine phosphate−sugar bond. [e] CPD III dimer of one nucleoside and one nucleotide with the inter-pyrimidine phosphate link present.

moments and CPD structures calculated with the HF method, which predicted the structures and dipole moments the best. The key structural parameters of the cyclobutane ring such as bond and torsion angles obtained by our group are very similar to those reported before and can be found in the Supporting Information.[51−53]

Discussion

The results demonstrate that binding of photolyase to a UV-p(dC)$_{10}$ substrate affects the physicochemical properties of the enzyme differently than binding to the UV-p(dT)$_{10}$ substrate. UV-p(dC)$_{10}$ induces a significantly smaller electrochromic shift and an almost negligible effect on the extinction coefficient of the $D_0 \rightarrow D_1$ transition. The effect of UV-p(dC)$_{10}$ on the resonance Raman spectrum is also much smaller. The largest difference was observed for the rate of charge recombination between $FADH^-$ and $Trp_{306}^{\bullet}$; it was faster with UV-p(dC)$_{10}$ substrate and slower for UV-p(dT)$_{10}$ substrate, both in comparison to free enzyme.[36] Despite these differences between binding of UV-p(dC)$_{10}$ and UV-p(dT)$_{10}$ substrates, their effect on the $FADH^-/FADH^{\bullet}$ reduction potential is the same within the margin of error.[37] In the remainder of the discussion, we will investigate the origin of the observed changes in these physicochemical properties of photolyase upon substrate binding.

Electrochromic Shift. MacFarlane and Stanley have pointed out that the permanent electric dipole moment of the CPD produces an electric field near the FAD cofactor in the enzyme−substrate complex that can explain the observed shift in the absorption spectrum of the oxidized FAD cofactor.[31] In previous work, we proposed that this electric dipole moment may explain the electrochromic shift in the $FADH^{\bullet}$ absorption spectrum along with the decrease in the rate of $FADH^- - Trp_{306}^{\bullet}$ charge recombination along with a small vibrational Stark effect also observed for $FADH^{\bullet}$ in the enzyme−UV-p(dT)$_{10}$ complex.[35,36]

To quantify the effect of the CPD electric dipole moment on the $FADH^{\bullet}$ properties, it is important to realize that both the strength and orientation of the dipole must contribute to the analysis. In this case, the electrochromic shift, ΔE, is given by[55]

$$\Delta E = -\frac{\Delta \vec{\mu}_1^{\,FADH^{\bullet}} \cdot \vec{F}_{CPD}}{hc} \qquad (1)$$

where $\Delta\vec{\mu}_1^{FADH^{\bullet}}$ is the difference dipole moment of the ground state and the first excited state of $FADH^{\bullet}$, $\vec{F}_{CPD}$ is the electric field produced by the CPD electric dipole moment, h is Planck's constant, and c is the speed of light. The orientation and strength of the electric dipole field of the CPD, $\vec{F}_{CPD}$, at point $\vec{r}$ is given by[56]

$$\vec{F}_{CPD} = \frac{1}{4\pi\varepsilon_r\varepsilon_0}\left[\frac{3(\vec{\mu}_{CPD}\cdot\vec{r})\vec{r}}{|\vec{r}|^5} - \frac{\vec{\mu}_{CPD}}{|\vec{r}|^3}\right] \qquad (2)$$

where $\vec{\mu}_{CPD}$ is the electric dipole moment of the CPD, $\vec{r}$ is the vector pointing from the center of C5A, C6A, C5B, and C6B (the "cyclobutane ring") to the center of the pyrazine ring of the flavin, $\varepsilon_0 = 8.85 \times 10^{-12}$ C^2 J^{-1} m^{-1} and ε_r is the relative dielectric constant of the medium.

Our calculations clearly show that the electric dipole moment of C[*c,s*]C is stronger than that of T[*c,s*]T, independent of the computational method and the specific structure of the CPD. The orientation of the electric dipole moment of cytosine and

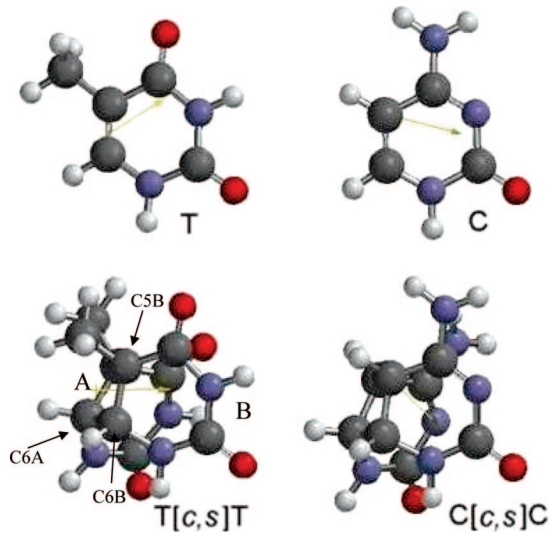

Figure 6. Hartree−Fock (3-21G* basis set) optimized geometries and electric dipole moments of thymine (T), cytosine (C), and of the thymine (T[*c,s*]T) and cytosine (C[*c,s*]C) *cis,syn*-cyclobutane dimers. Although the dipole moment is shown in the figure pointing from the positive end to the negative end of the charge displacement (faint yellow arrow), we used the conventional orientation from the negative end to positive end of the charge displacement in our calculations.

of C[*c,s*]C is quite different from that of thymine and T[*c,s*]T, respectively (Figure 6). Since the electric dipole moments that were calculated with the HF method reproduce the experimentally determined and estimated values the most accurately,[31,38,39] we will use the results of CPD III that were obtained with the HF method for the analysis of our experimental results. This model assumes that the Coulomb contributions of the other backbone phosphates are canceled due to interactions with positively charged residues at the protein surface.[28,33,34]

In their computational study of the T[*c,s*]T nucleobase dimer, Aida et al. labeled the two thymines A and B to distinguish their structural properties.[52] We will use the same notation, as indicated in Figure 6. The orientation of the electric dipole moment can be defined with respect to the framework of CPD III and a plane through the C6A, C5A, and C5B atoms. The C5A atom is arbitrarily chosen as the origin. The normal to this plane is calculated so that it points away from the sugar and phosphate groups. In Table 3, we list the angle of the electric dipole moment with respect to the normal to this plane and the angles of the projection of the electric dipole moment onto this plane with the vectors pointing from C5A to C6A and from C5A to C5B. We also provide the distance of C6B to the C6A−C5A−C−5B plane as a measure of the puckering of the cyclobutane ring. These simple calculations provide a quantitative picture of the orientation of the electric dipole moments of T[*c,s*]T and C[*c,s*]C. The T[*c,s*]T electric dipole moment is nearly parallel to the normal with a 5.6° angle while this angle is 33.1° for the electric dipole moment of C[*c,s*]C. The projection of either dipole moment onto the C6A−C5A−C−5B plane has only a small contribution along the C5A−C5B vector. The T[*c,s*]T dipole moment also has only a small projection along the C5A−C6A vector. In contrast to this, the projection of the C[*c,s*]C dipole moment makes an angle of 177.6° with the C5A−CA6 vector and a projection length of 8.7 D. Therefore, the T[*c,s*]T electric dipole moment lies almost entirely along the normal of the C5B−C5A−C6A plane, while that of C[*c,s*]C makes an angle of 33° with this normal and lies mainly in the plane described by the normal and the C5A−C6A vector. Both dipole moments point away from the phosphate and sugar

TABLE 3: Orientation of Dipole Moment of CPD III Calculated with the HF Methodology with Respect to C6A−C5A−C5B Plane and Puckering of the Cyclobutane Ring (the Distance between C6B and the C6A−C5A−C5B Plane)

CPD	angle (deg) with normal[a]	angle (deg) with C5A → C6A[c]	angle (deg) with C5A → C5B[c]	angle (deg) C6A−C5A−C5B	distance (Å) between C6B and plane[d]
thymine	5.6 (8.6)[b]	51.3 (0.52)[b]	138.6 (0.63)[b]	87.2	0.61
cytosine	33.1 (13.4)[b]	177.6 (8.7)[b]	95.1 (0.77)[b]	87.5	0.52
structure[e]	N.A.	N.A.	N.A.	86.4	0.65

[a] The normal of the C6A−C5A−C5B plane points away from the sugar and phosphate moieties. [b] The number between parentheses represents the length of the dipole moment in debye along each line. [c] Angle with the projection of the dipole moment onto the C6A−C5A−C5B plane. [d] C6B lies below the C6A−C5A−C5B plane toward the sugar and phosphate moieties. [e] Coordinates are from strand I, T7(thymine A) and TCP8(thymine B), PDB entry 1TEZ.[34]

TABLE 4: Calculated Electrochromic Shift (cm^{-1}) of the $D_0 \rightarrow D_1$ Transition of $FADH^{\bullet}$ Induced by the Electric Dipolar Fields of T<>T and C<>C for Different Orientations of the Difference Dipole Vector, $\Delta\vec{\mu}_1$, and for Different Values of ε_r

		calculated electrochromic shift (cm^{-1}) for different orientations of $\Delta\vec{\mu}_1$				
	ε_r	N3 → C2	N3 → N1	N3 → C10a	N3 → N10	N3 → C9a
T<>T	1	−49	−16	+21	+20	+42
T<>T	3	−16	−5	+7	+7	+14
C<>C	1	−326	−306	−203	−204	−129
C<>C	3	−108	−102	−68	−68	−43

groups. In the calculations, their orientation was taken to point from the negative end to the positive end of the charge displacement.

The crystal structure of *A. nidulans* in complex with a repaired CPD analogue provides the best framework to estimate the effect of the CPD electric dipole moment on the FAD cofactor. Table 3 also lists the data for the framework of the thymines in the crystal structure. The finding that the C6A−C5A−C5B angle and the C6B pucker are very similar to the values calculated for T[*c,s*]T and C[*c,s*]C indicates that the crystal structure provides a good framework for our calculations. The final pieces of the puzzle are the strength and direction of the difference dipole moment of the oxidized flavin in photolyase as determined by MacFarlane and Stanley.[31] Since the electrochromic shift observed for $FADH^{\bullet}$ is of a similar magnitude compared to that for FAD_{ox},[31,35] we assume that the difference dipole moment of $FADH^{\bullet}$ is similar to that of FAD_{ox}. This is a reasonable assumption because the binding geometry of T<>T is most likely independent of the FAD oxidation state, and its electric dipole moment produces a very similar electric dipole field in both cases. MacFarlane and Stanley reported the strength of the difference dipole to be 4.0 D.[31] The direction of the electric dipole field at the flavin cofactor is calculated using eq 2 with $\vec{r}$ pointing from the center of "cyclobutane" ring to the center of the pyrazine ring of the flavin. The distance between these two centers is 10.1 Å.

By entering all the available information into eqs 1 and 2, we find that the maximum electrochromic shift is $-175\cos(\Delta_1)$ cm^{-1} and $-360\cos(\Delta_2)$ cm^{-1} in the presence of T[*c,s*]T and C[*c,s*]C, respectively. These values have been calculated for $\varepsilon_r = 1$, and Δ_1 and Δ_2 are the angles between the direction of the electric dipole field vector ($\vec{r}$) at the flavin and $\Delta\vec{\mu}_1^{FAD}$ for T[*c,s*]T and C[*c,s*]C, respectively. The difference dipole vector of FAD_{ox}, $\Delta\vec{\mu}_1^{FAD}$, has been estimated to lie almost along the line from N3 to N1.[31] We have calculated the electrochromic shift for several different orientations of the difference dipole moment, and the results are listed in Table 4. Using all the values exactly and placing the difference dipole vector along the N3−N1 line slightly between N1 and C2, it is clear that a negative value of the electrochromic shift is obtained for binding of T[*c,s*]T. A positive electrochromic shift can be obtained by rotating the difference dipole vector by about 10° counterclockwise to fall along the N3−C10a line. By rotating the difference dipole moment by about 20° counterclockwise to point along the N3−C9a line, we calculate an electrochromic shift of +42 and +14 cm^{-1} for $\varepsilon_r = 1$ and $\varepsilon_r = 3$, respectively. These values compare quite well to the experimentally determined value of $\Delta E = +80$ cm^{-1} upon binding of UV-$p(dT)_{10}$.[35]

The validity of our calculation of the T[*c,s*]T structure and electric dipole moment is strongly supported by the fact that we can calculate the electrochromic shift with the correct sign and order of magnitude after only a small change in the angle between this dipole moment and the $FADH^{\bullet}$ difference dipole moment. It also provides evidence that the observed shift in the $FADH^{\bullet}$ absorbance spectrum upon binding of photolyase to UV-$p(dT)_{10}$ is an electrochromic shift induced by the electric dipole field of the substrate as previously proposed.[31] Finally, it indicates that also our calculated structure and dipole moment of C[*c,s*]C are sound. Since the observed shift induced by C[*c,s*]C is poorly predicted by the electrochromic shift calculation, we interpret this result as evidence that the C[*c,s*]C binding geometry in the enzyme−substrate complex is quite different from that of the T[*c,s*]T substrate. Therefore, despite its significantly stronger electric dipole moment, the orientation of the C[*c,s*]C electric dipole moment, its distance from the $FADH^{\bullet}$, or both are unfavorable to produce any significant electrochromic shift of the absorption spectrum of $FADH^{\bullet}$. The different binding geometry of C[*c,s*]C could also explain the lower binding affinity of photolyase for UV-$oligo(dC)_{12-18}$ compared to UV-$oligo(dT)_{12-18}$.[40]

Charge Recombination. Although the binding geometry of a C[*c,s*]C lesion to photolyase is not yet known, a qualitative analysis of the effect of substrate binding on the rate of the $FADH^-$ to $Trp_{306}^{\bullet}$ charge recombination can still be given. The rate of electron transfer, k_{et}, is given by[57−59]

$$k_{et} = \sqrt{\frac{4\pi^3}{h^2\lambda k_B T}} H_{AB}{}^2 \exp\left[-\frac{(\Delta G^\circ + \lambda)^2}{4\lambda k_B T}\right] \qquad (3)$$

where H_{AB} is the electronic coupling matrix element, ΔG° is the change in standard free energy, λ is the reorganization energy, k_B is Boltzmann's constant, and T is the temperature. In the case of the charge recombination, the change in standard free energy is given by

$$\Delta G^\circ = e[E_m(FADH^-/FADH^{\bullet}) - E_m(Trp^{\bullet}/TrpH)] \qquad (4)$$

Upon substrate binding, ΔG° is modified in two ways. First, the $FADH^-/FADH^{\bullet}$ reduction potential increases by an amount of $\Delta E_m(FADH^-/FADH^{\bullet}) \approx 70$ mV. Second, the interaction of

the electric field of the substrate dipole moment with the reactants and products of the electron transfer reaction modifies $\Delta G°$ by ΔU. In the enzyme−substrate complex, the change in standard free energy is given by

$$\Delta G°(\text{complex}) = \Delta G° + e\Delta E_{\text{m}}(\text{FADH}^-/\text{FADH}^\bullet) + \Delta U \quad (5)$$

For the charge-recombination reaction, the products are charge neutral, and only one of the reactants, $FADH^-$, is charged. In this case, $\Delta U = \vec{E}\cdot(2q\vec{r}_{\text{et}})$,[60] and the sign and magnitude depend on the orientation and strength of the applied electric field, $\vec{E}$, with respect to the direction vector of the electron transfer, $\vec{r}_{\text{et}}$, while q is the amount of charge being transferred.

Since binding of UV-p$(dT)_{10}$ and UV-p$(dC)_{10}$ to photolyase raises the $FADH^-/FADH^\bullet$ reduction potential by the same amount within the experimental error, the difference in k_{et} between both enzyme−substrate complexes is mainly due to a difference in ΔU. In an earlier study, we argued that the charge-recombination process occurs in the normal region. The fact that binding of UV-p$(dC)_{10}$ to photolyase increases the rate of charge recombination suggests that $\Delta U_{C<>C} < 0$ in this case. On the other hand, binding of UV-p$(dT)_{10}$ to photolyase decreases the rate of charge recombination indicating that $\Delta U_{T<>T} > 0$. The opposite sign of ΔU for these two substrates can only be explained by the difference in orientation of the dipole electric field that the substrate dipole moments generate near the FAD cofactor. Our analysis predicts that the angle between the electric field generated by T[*c,s*]T and $\vec{r}_{\text{et}}$ is between 0° and 90°, while the same angle is between 90° and 180° for the C[*c,s*]C lesion. The important finding of this analysis is that the difference between the effects of these two substrates on the rate of charge recombination can only be explained by the different electric dipole fields generated by these substrates. This strongly supports the earlier suggestion that the substrate electric field affects the rate of charge recombination and may also play an important role in efficiency of DNA repair by modifying the electron transfer from the $FADH^-$ singlet excited-state to the CPD.

$FADH^-/FADH^\bullet$ Reduction Potential. The $FADH^-/FADH^\bullet$ reduction potential of DNA photolyase increases ~70 mV upon binding of either UV-p$(dT)_{10}$ or UV-p$(dC)_{10}$. A number of factors appear to influence the reduction potential of the FAD cofactor in a protein including hydrogen bonding, π-stacking, dehydration, and conformational changes to the isoalloxazine ring.[61−67] From our Raman data, we conclude that hydrogen bonding to the FAD cofactor is altered less with the UV-p$(dC)_{10}$ compared to the UV-p$(dT)_{10}$ substrate, so changes in hydrogen bonding may not be the strongest influence on the increase in reduction potential. A more likely candidate for the alteration may be the conformation of the isoalloxazine ring; a computational paper by Walsh and Miller and a study of model compounds implicate the planarity of the isoalloxazine ring as one influence on the modification in the $FADH^-/FADH^\bullet$ reduction potential.[66,67] Mees et al. report that the isoalloxazine ring is bent ~9° when substrate is bound to *A. nidulans* DNA photolyase (comparison of crystal structures 1TEZ and 1QNF).[34] The bend would destabilize the neutral semiquinone radical relative to the fully reduced state, leading to an increase in the reduction potential. We are unable to detect the occurrence of the bend due to poor signal-to-noise of the photolyase−UV-p$(dC)_{10}$ Raman spectrum. Furthermore, calculations suggest that the out-of-plane normal modes that may become enhanced upon bending of the isoalloxazine ring will most likely appear in the low-frequency region of the resonance Raman spectrum (Eisenberg, A.; Schelvis, J. P. M., unpublished results), which was not recorded for this specific study. Finally, it is possible that the electric dipole moment modifies the $FADH^-/FADH^\bullet$ reduction potential by altering the energy states near the ionization limit of $FADH^\bullet$. However, the fact that the T[*c,s*]T and C[*c,s*]C have significantly different dipole moments but induce a similar change in the reduction potential all but seems to rule out this possibility.

Quantum Efficiency of CPD Repair. Kim and Sancar have shown that photolyase has an 8-fold lower affinity for UV-oligo$(dC)_{12-18}$ compared to UV-oligo$(dT)_{12-18}$ and that UV-oligo$(dC)_{12-18}$ is repaired with an 18-fold lower quantum yield than UV-oligo$(dT)_{12-18}$.[40] We demonstrate that the electric dipole moments of T[*c,s*]T and C[*c,s*]C affect the electronic energy levels of $FADH^\bullet$ as well as the rate of charge recombination between $FADH^-$ and $Trp_{306}^\bullet$ differently. The most important parameter for the kinetics and thermodynamics of DNA repair is the reduction potential of the $FADH^-/FADH^\bullet$ couple. Our results show that binding of UV-p$(dT)_{10}$ and of UV-p$(dC)_{10}$ modify this reduction potential in a similar way within the margin of experimental error. The latter result suggests that the electron transfer from the singlet excited state of $FADH^-$ to the CPD in the DNA repair step has a similar standard free energy for both T[*c,s*]T and C[*c,s*]C, especially since model compound studies indicate that T[*c,s*]T and C[*c,s*]C have similar reduction potentials.[68] However, it should be kept in mind that we have measured the $FADH^\bullet/FADH^-$ reduction potential in the ground state, while the forward electron transfer from $FADH^-$ to the CPD occurs from the $FADH^-$ singlet excited state. Furthermore, the charge recombination experiments demonstrate that the substrate electric dipole field can modify the change in free energy of electron transfer reactions in photolyase, even though the reduction potentials do not change.

Kim and Sancar have proposed that the difference in repair efficiency of T[*c,s*]T and C[*c,s*]C is related to the position of the radical on the CPD.[40] In the case of $T[c,s]T^{\bullet-}$, the radical would be localized at C(4) in close proximity to the cyclobutane ring. In contrast, the radical would be localized at C(2) of $C[c,s]C^{\bullet-}$ farther away from the cyclobutane ring. However, at this point, it cannot be ruled out that a difference in binding geometry between T[*c,s*]T and C[*c,s*]C modifies the electron transfer pathway from $FADH^-$ to C[*c,s*]C and/or the distance between $FADH^-$ to C[*c,s*]C. Such a change could result in a slower rate of forward electron transfer to the C[*c,s*]C, leading to a competition between reductive cleavage of the cyclobutane ring and unproductive charge recombination between $C[c,s]C^{\bullet-}$ and $FADH^\bullet$. Finally, the importance of the CPD electric dipole moment in stabilizing the $CPD^{\bullet-}-FADH^\bullet$ charge-separated state prior to reductive cleavage of the cyclobutane ring may also be an important factor that contributes to efficient CPD repair by photolyase.[31] Therefore, the differences in electric dipole moment properties between T[*c,s*]T and C[*c,s*]C may also affect the quantum yield of repair for each CPD differently.

Conclusions

Our experiments demonstrate that binding of T[*c,s*]T-containing DNA and of C[*c,s*]C-containing DNA affect the physicochemical properties of photolyase differently, with the exception of the $FADH^-/FADH^\bullet$ reduction potential. The finding that the calculated electrochromic shift is in close agreement with the experimentally determined blue shift in the $FADH^\bullet$ absorption spectrum in the photolyase−UV-p$(dT)_{10}$ complex indicates that

our calculated electric dipole moments are valid and that the interaction between the electric dipole moment and those of the FAD cofactor can satisfactorily explain the observed blue shift in the $FADH^{\bullet}$ absorption spectrum as an electrochromic shift with perhaps a small contribution due to dehydration of the active site. The finding that the electrochemical shift calculation fails for the photolyase−UV-p$(dC)_{10}$ strongly suggests that the binding geometry of the C[*c,s*]C lesion is different from that of the T[*c,s*]T lesion.

The finding that the $FADH^{-}/FADH^{\bullet}$ reduction potential increases by a similar amount upon binding of photolyase to either substrate appears to rule out that modification of hydrogen bonding between $FADH^{\bullet}$ and its protein environment is the main contributor to this increase in reduction potential. We propose that the observed bend in the isoalloxazine ring upon substrate binding may be a key contributor in raising the $FADH^{-}/FADH^{\bullet}$ reduction potential, but other factors such as dehydration of the binding pocket cannot be ruled out. Since the reduction potential is the same in the photolyase−UV-p$(dT)_{10}$ and −UV-p$(dC)_{10}$ complexes, it does not explain the differences in repair efficiencies of photolyase for T[*c,s*]T and C[*c,s*]C lesions. However, the electron transfer to the CPD occurs from the $FADH^{-}$ singlet excited state ($^1FADH^{-}$), and the effect of substrate binding on the $^1FADH^{-}/FADH^{\bullet}$ reduction potential may be different. Finally, the importance of the CPD electric dipole moment in stabilizing the $CPD^{\bullet -}-FADH^{\bullet}$ charge-separated state prior to reductive cleavage of the cyclobutane ring may also be an important factor that contributes to efficient CPD repair by photolyase.

Acknowledgment. The research was sponsored by NSF Grants MCB 0415611 and 0742122 (J.P.M.S.), the Faculty Scholarship Program at Montclair State University (J.P.M.S.), and by an EXCEL Fellowship from Lafayette College (M.T.). All experiments were done at New York University and at Lafayette College. Part of the data analysis was done at Montclair State University.

Supporting Information Available: Structures of the pyrimidine bases and their cyclobutane dimers, several AM1 and HF optimized geometries, a table with deconvolution parameters, and tables with bond angles and torsion angles of optimized CPDs. This material is available free of charge via the Internet at http://pubs.acs.org.

References and Notes

(1) Perdiz, D.; Grof, P.; Mezzina, M.; Nikaido, O.; Moustacchi, E.; Sage, E. *J. Biol. Chem.* **2000**, *275*, 26732.
(2) Douki, T.; Reynaud-Angelin, A.; Cadet, J.; Sage, E. *Biochemistry* **2003**, *42*, 9221.
(3) Mouret, S.; Baudouin, C.; Charveron, M.; Favier, A.; Cadet, J.; Douki, T. *Proc. Natl. Acad. Sci. U.S.A.* **2006**, *103*, 13765.
(4) You, Y.; Lee, D.; Yoon, J.; Nakajima, S.; Yasui, A.; Pfeifer, G. P. *J. Biol. Chem.* **2001**, *276*, 44688.
(5) Mitchell, D. L.; Jen, J.; Cleaver, J. E. *Nucleic Acids Res.* **1992**, *20*, 225.
(6) Frederico, L. A.; Kunkel, T. A.; Shaw, B. R. *Biochemistry* **1990**, *29*, 2532.
(7) Taylor, J. S. *Acc. Chem. Res.* **1994**, *27*, 76.
(8) Peng, W.; Shaw, B. R. *Biochemistry* **1996**, *35*, 10172.
(9) Brash, D.; Rudolph, J.; Simon, J.; Lin, A.; McKenna, G.; Baden, H.; Halperin, A.; Poten, J. *Proc. Natl. Acad. Sci. U.S.A.* **1991**, *88*, 10124.
(10) Christmann, M.; Tomicic, M. T.; Roos, W. P.; Kaina, B. *Toxicology* **2003**, *193*, 3.
(11) Hemminki, K.; Xu, G.; Kause, L.; Koulu, L. M.; Zhao, C.; Jansen, C. T. *Carcinogenesis* **2002**, *23*, 605.
(12) Sancar, A. *Chem. Rev.* **2003**, *103*, 2203.
(13) Johnson, J. L.; Hamm-Alvarez, S.; Payne, G.; Sancar, G. B.; Rajagopalan, K. V.; Sancar, A. *Proc. Natl. Acad. Sci. U.S.A.* **1988**, *85*, 2046.
(14) Jorns, M. S.; Sancar, G. B.; Sancar, A. *Biochemistry* **1984**, *23*, 2673.
(15) Gindt, Y. M.; Vollenbroek, E.; Westphal, K.; Sackett, H.; Sancar, A.; Babcock, G. T. *Biochemistry* **1999**, *38*, 3857.
(16) Sancar, G. B.; Jorns, M. S.; Payne, G.; Fluke, D. J.; Rupert, C. S.; Sancar, A. *J. Biol. Chem.* **1987**, *262*, 492.
(17) Heelis, P. F.; Payne, G.; Sancar, A. *Biochemistry* **1987**, *26*, 4634.
(18) Weber, S. *Biochim. Biophys. Acta* **2005**, *1707*, 1.
(19) Aubert, C.; Vos, M. H.; Mathis, P.; Eker, A. P. M. *Nature (London)* **2000**, *405*, 586.
(20) Byrdin, M.; Eker, A. P. M.; Vos, M. H.; Brettel, K. *Proc. Natl. Acad. Sci. U.S.A.* **2003**, *100*, 8676.
(21) Wang, H.; Saxena, C.; Quan, D.; Sancar, A.; Zhong, D. *J. Phys. Chem. B* **2005**, *109*, 1329.
(22) Heelis, P. F.; Sancar, A. *Biochemistry* **1986**, *25*, 8163.
(23) Li, Y. F.; Heelis, P. F.; Sancar, A. *Biochemistry* **1991**, *30*, 6322.
(24) Kavakli, I. H.; Sancar, A. *Biochemistry* **2004**, *43*, 15103.
(25) Park, H. W.; Kim, S. T.; Sancar, A.; Deisenhofer, J. *Science* **1995**, *268*, 1866.
(26) Tamada, T.; Kitadokoro, K.; Higuchi, Y.; Inaka, K.; Yasui, A.; de Ruiter, P. E.; Eker, A. P. M.; Miki, K. *Nat. Struct. Biol.* **1997**, *4*, 887.
(27) Komori, H.; Masui, R.; Kuramitsu, S.; Yokoyama, S.; Shibata, T.; Inoue, Y.; Miki, K. *Proc. Natl. Acad. Sci. U.S.A.* **2001**, *98*, 13560.
(28) VandeBerg, B. J.; Sancar, G. B. *J. Biol. Chem.* **1998**, *273*, 20276.
(29) Sanders, D. B.; Wiest, O. *J. Am. Chem. Soc.* **1999**, *121*, 5127.
(30) Antony, J.; Medvedev, M.; Stuchebruhkov, A. A. *J. Am. Chem. Soc.* **2000**, *122*, 1057.
(31) MacFarlane, A. W. IV.; Stanley, R. J. *Biochemistry* **2001**, *40*, 15203.
(32) Christine, K. S.; MacFarlane, A. W., IV.; Yang, K.; Stanley, R. J. *J. Biol. Chem.* **2002**, *277*, 38339.
(33) Torizawa, T.; Ueda, T.; Kuramitsu, S.; Hitomi, K.; Todo, T.; Iwai, S.; Morikawa, K.; Shimada, I. *J. Biol. Chem.* **2004**, *279*, 32950.
(34) Mees, A.; Klar, T.; Gnau, P.; Hennecke, U.; Eker, A. P. M.; Carell, T.; Essen, L. *Science* **2004**, *306*, 1789.
(35) Schelvis, J. P. M.; Ramsey, M.; Sokolova, O.; Tavares, C.; Cecala, C.; Connell, K.; Wagner, S.; Gindt, Y. M. *J. Phys. Chem. B* **2003**, *107*, 12352.
(36) Kapetanaki, S. M.; Ramsey, M.; Gindt, Y. M.; Schelvis, J. P. M. *J. Am. Chem. Soc.* **2004**, *126*, 6214.
(37) Gindt, Y. M.; Schelvis, J. P. M.; Thoren, K. L.; Huang, T. H. *J. Am. Chem. Soc.* **2005**, *127*, 10472.
(38) Kulakowska, I.; Rabczenko, A. *Biochim. Biophys. Acta* **1974**, *361*, 131.
(39) Kulakowska, I.; Geller, M.; Lesyng, B.; Wierzchowski, K. L. *Biochim. Biophys. Acta* **1974**, *361*, 119.
(40) Kim, S.-T.; Sancar, A. *Biochemistry* **1991**, *30*, 8623.
(41) Husain, I.; Sancar, A. *Nucleic Acids Res.* **1987**, *15*, 1109.
(42) Sokolova, O.; Cecala, C.; Gopal, A.; Cortazar, F.; McDowell-Buchanan, C.; Sancar, A.; Gindt, Y. M.; Schelvis, J. P. M. *Biochemistry* **2007**, *46*, 3673.
(43) Murgida, D. H.; Schleicher, E.; Bacher, A.; Richter, G.; Hildebrandt, P. *J. Raman Spectrosc.* **2001**, *32*, 551.
(44) Li, J.; Uchida, T.; Todo, T.; Kitagawa, T. *J. Biol. Chem.* **2006**, *281*, 25551.
(45) Byrdin, M.; Sartor, V.; Eker, A. P. M.; Vos, M. H.; Aubert, C.; Brettel, K.; Mathis, P. *Biochim. Biophys. Acta* **2004**, *1655*, 64.
(46) Wang, B.; Jorns, M. S. *Biochemistry* **1989**, *28*, 1148.
(47) Desfrancois, C.; Abdoul-Carime, H.; Carles, S.; Periquet, V.; Schermann, J. P.; Smith, D. M. A.; Adamowicz, L. *J. Chem. Phys.* **1999**, *110*, 11876.
(48) Li, J.; Cramer, J. J.; Truhlar, D. G. *Biophys. Chem.* **1999**, *78*, 147.
(49) Bakalarski, G.; Grochowski, P.; Kwiatkowski, J. S.; Lesyng, B.; Leszczyiiskii, *J. Chem. Phys.* **1996**, *204*, 301.
(50) Civcir, P. U. *J. Mol. Struct.: THEOCHEM* **2000**, *532*, 157.
(51) Durbeej, B.; Eriksson, L. A.; Durbeej, B.; Eriksson, L. A. *J. Am. Chem. Soc.* **2000**, *122*, 10126.
(52) Aida, M.; Inoue, F.; Kaneko, M.; Dupuis, M. *J. Am. Chem. Soc.* **1997**, *119*, 12274.
(53) Li, Z.; Eriksson, L. A. *Chem. Phys. Lett.* **2005**, *401*, 99.
(54) Park, H.; Zhang, K.; Ren, Y.; Nadji, S.; Sinha, N.; Taylor, J.-S.; Kang, C. *Proc. Natl. Acad. Sci. U.S.A.* **2002**, *99*, 15965.
(55) Liptay, W. *Angew. Chem., Int. Ed.* **1969**, *8*, 177.
(56) Lorrain, P.; Corson, D. R. In *Electromagnetism: Principles and Applications*; W.H. Freeman and Co.: New York, 1979.
(57) Marcus, R. A.; Sutin, N. *Biochim. Biophys. Acta* **1985**, *811*, 265.
(58) Gray, H. B.; Winkler, J. R. In *Electron Transfer in Chemistry*; Balzani, V., Ed.; Weinheim: New York, 2001; p 3.
(59) Page, C. C.; Moser, C. C.; Chen, X.; Dutton, P. L. *Nature (London)* **1999**, *402*, 47.
(60) Shin, Y. K.; Brunschwig, B. S.; Creutz, C.; Sutin, N. *J. Am. Chem. Soc.* **1995**, *117*, 8668.
(61) Pellet, J. D.; Sabaj, K. M.; Stephens, A. W.; Bell, A. F.; Wu, J.; Tonge, P. J.; Stankovich, M. T. *Biochemistry* **2000**, *39*, 13982.

(62) Breinlinger, E.; Niemz, A.; Rotello, V. M. *J. Am. Chem. Soc.* **1995**, *117*, 5379.

(63) Cuello, A. O.; McIntosh, C. M.; Rotello, V. M. *J. Am. Chem. Soc.* **2000**, *122*, 3517.

(64) Swenson, R. P.; Krey, G. D. *Biochemistry* **1994**, *33*, 8505.

(65) Breinlinger, E. C.; Rotello, V. M. *J. Am. Chem. Soc.* **1997**, *119*, 1165.

(66) Walsh, J. D.; Miller, A.-F. *J. Mol. Struc.: THEOCHEM.* **2003**, *623*, 185.

(67) Hasford, J. J.; Kemnitzer, W.; Rizzo, C. J. *J. Org. Chem.* **1997**, *62*, 5244.

(68) Scannell, M. P.; Fenick, D. J.; Yeh, S.-R.; Falvey, D. E. *J. Am. Chem. Soc.* **1997**, *119*, 1971.

JP806526Y